

NEW STUDIES ON THE ASPECTS
OF NUCLEAR SHAPES*F.R. XU^a, H.L. LIU^{a,b}, Y. SHI^{c,d,e}, H.L. WANG^a, P.M. WALKER^f
S. FRAUENDORF^g, J.C. PEI^{a,c,d}^aSchool of Physics, Peking University, Beijing 100871, China^bDept. of Applied Physics, Xi'an Jiaotong University, Xi'an 710049, China^cDept. of Physics and Astronomy, University of Tennessee
Knoxville, Tennessee 37996, USA^dPhysics Division, Oak Ridge National Laboratory

Post Office Box 2008, Oak Ridge, Tennessee 37831, USA

^eDept. of Physics, University of Jyväskylä, P.O. Box 35, 40014 Jyväskylä, Finland^fDept. of Physics, University of Surrey, Guildford, Surrey GU2 7XH, UK^gDept. of Physics, University of Notre Dame, Notre Dame, Indiana 46556, USA*(Received December 19, 2012)*

Using the pairing-deformation-frequency self-consistent total-Routhian-surface and configuration-constrained potential-energy-surface calculations, we have studied nuclear deformation and its effect on the structure of nuclei. It was found that the high-order multipolarity-six (β_6) deformation plays a significant role in superheavy nuclei. Possible non-collective high-spin isomeric states which locate in the second well of actinide nuclei have been investigated with the predictions of excitation energies and configurations. High-spin isomers can extend shape coexistence in $A \sim 190$ neutron-deficient nuclei. Triaxiality with $\gamma \sim 30^\circ$ is found in the ground and excited rotational states of the $A \sim 70$ germanium isotopes. Octupole correlations have also been discussed in different mass regions. In recent experiments, the textbook nucleus ^{158}Er has been reached at ultrahigh spins around $65\hbar$. We have studied ^{158}Er ultrahigh-spin states by means of the self-consistent tilted-axis-tilting method based on the Nilsson shell correction and the Skyrme-Hartree-Fock model. The calculation with a $\gamma \approx 12^\circ$ triaxial-strongly-deformed (TSD) excited configuration can well reproduce the observed large transitional quadrupole moment. It is demonstrated that the TSD minimum at negative γ deformation which appears in the principal-axis-tilting approach is a saddle point if allowing the rotational axis to change direction.

DOI:10.5506/APhysPolB.44.271

PACS numbers: 21.10.Re, 21.10.Ky, 21.60.Cs, 23.20.Lv

* Presented at the Zakopane Conference on Nuclear Physics "Extremes of the Nuclear Landscape", Zakopane, Poland, August 27–September 2, 2012.

1. Introduction

Nuclear shape is an essential property of nucleus. A systematic investigation based on the Nilsson potential has suggested that about 85% of nuclides are prolate in their ground states [1]. The deformation and incurred effects originate from the fillings of high- j orbits. As seen in the deformed diagrams of single-particle levels, high- j low- Ω orbits have strong prolate-driving force, while high- j high- Ω orbits drive nucleus towards oblate shape. For certain numbers of protons and neutrons, however, nuclei can have various coexisting shapes. For example, experiment addressed that the lowest three 0^+ states observed in the neutron-deficient nucleus ^{186}Pb are spherical, oblate and prolate [2]. Nuclear shape can be also changed by particle-hole excitation, broken-pair excitation and rotational motion.

Usually, the axially symmetric quadrupole deformation (*i.e.*, β_2) is dominant, but other types of deformations can play important roles in the determination of nuclear properties. Triaxial deformation results in the specific features of the associated rotational bands, such as wobbling [3], spin-chirality [4] and signature-inversion [5–7] rotations. Octupole deformation leads to enhanced $E1$ transitions connecting interleaved positive- and negative-parity bands, which is similar to rotational bands observed in reflection-asymmetric molecules [8]. The inclusion of hexadecapole deformation can significantly improve the calculations of collective rotations. It has been found that the multipolarity-six deformation plays an important role in stabilizing superheavy nuclei, which leads to enlarged shell gaps [9, 10]. The nucleus, ^{158}Er , has been claimed to undergo a beautiful shape evolution from prolate via oblate to triaxial strong deformation, with increasing rotational angular momentum from $I = 0$ to ≈ 65 [11, 12].

2. Calculations and discussions

In the past years, we studied various deformations for different mass regions, using different models including the cranked Woods–Saxon, configuration-constrained potential energy surface and tilted cranked Skyrme–Hartree–Fock. The β_6 deformation was seen in superheavy nuclei. Highly-elongated high- K fission isomers were found in actinide nuclei. The β_3 deformation or β_3 softness was studied as well. Triaxial deformations in $A \sim 70$ nuclei and in ^{158}Er at ultrahigh spins were investigated.

2.1. The multipolarity-six β_6 deformation in superheavy nuclei

Superheavy nuclei have been predicted to have various shapes including spherical, axial and triaxial deformations, with possible shape isomers existing [13, 14]. It has been well known that deformations can change the shell

fillings of single-particle orbits and hence result in the changes of nuclear properties. The deformation information can be obtained in many cases by spectroscopy in experiment. For example, in ^{254}No a quadrupole deformation of $\beta_2 \approx 0.27$ has been extracted from the measured ground-state band [15]. It is of special interest that high-order deformations are remarkable in superheavy mass region [16, 17]. The inclusion of the β_6 deformation brings an extra binding energy of more than 1 MeV, giving an improved reproduction of experimental masses [16]. Large β_6 deformation has been predicted in the $A \approx 250$ mass region [18].

It is hard to extract direct information about high-order deformations. However, we found that we can analyze high-order deformations and their effects by calculating the excitation energies of broken-pair isomeric states. The broken-pair excitation energy is sensitive to the level spacing of single-particle orbits. We have performed Woods–Saxon potential-energy-surface (PES) calculations with the inclusion of the multipolarity-six deformation β_6 [9]. An approximate particle-number projection was employed by means of the Lipkin–Nogami method with pairing strengths determined by the average gap method. The details can be found in Ref. [9].

As commented above, ^{254}No is a good example for the study of deformation and its effects, in which high-spin states with $I \leq 20\hbar$ [15, 19] and broken-pair multi-quasiparticle (multi-qp) isomers [20, 21] have been observed. The PES calculation for the ^{254}No ground state gives a deformation of ($\beta_2 = 0.25$, $\beta_4 = 0.011$) with $\beta_6 = -0.03$. Due to the β_6 deformation, our calculations give enlarged $Z = 100$ and $N = 152$ deformed shell gaps (increased by 0.5 and 0.2 MeV, respectively) [9], which enhances the stabilities of superheavy nuclei around the $Z = 100$ and $N = 152$ shells, evidenced already by experiments [22]. The multipolarity-six deformation also brings an extra binding energy of 0.8 MeV to the ground state of ^{254}No [9]. Multi-qp high- K isomer is a sensitive probe into the level spacing of single-particle orbits. We found that β_6 has a remarkable effect on level spacing. In order to include the shape polarization effect from the single-particle orbits which specify the configuration of a given multi-qp state, we have performed configuration-constrained PES calculations [23]. Several 2-qp and 4-qp isomers have been observed in ^{254}No [20, 24]. It was found that excitation energy calculations with the inclusion of the β_6 deformation are much better than calculations without β_6 , compared with the data of the observed isomers, see Ref. [9]. Calculations with β_6 reproduce well the experimental energies of the observed 2-qp and 4-qp isomers, see Ref. [9].

The moment of inertia is another sensitive probe into the deformation of rotational states. It is amazing why ^{254}No has a slower rotational alignment than its neighboring even isotope ^{252}No , which were observed experimentally [15, 19, 25]. For collective rotation, we have performed the pairing-

deformation-frequency self-consistent cranked Woods–Saxon calculation in the $(\beta_2, \beta_4, \beta_6, \beta_8)$ deformation space [10] with quadrupole pairings considered [26]. Calculations incorporating high-order deformations reproduce well the observed fast alignment in ^{252}No and slow alignment in ^{254}No [10]. The ^{254}No has a slightly larger β_6 deformation than ^{252}No [10]. We found that the β_6 deformation mainly influences the rotational alignment of the neutrons [10]. The neutron Fermi surface in ^{254}No locates just in the $N = 152$ deformed shell. Our calculations show that the rotational alignments of the nuclei with neutron Fermi surfaces in or above the $N = 152$ shell are delayed due to the presence of the β_6 deformation, while the alignments of nuclei with neutron Fermi surfaces below the $N = 152$ shell are not or less influenced [10]. Figure 1 displays the slower rotational alignments calculated with the inclusion of high-order deformations in nuclei with $N = 152$, compared with those with $N = 150$. The slow alignments are due to the β_6 deformation (β_8 is less important).

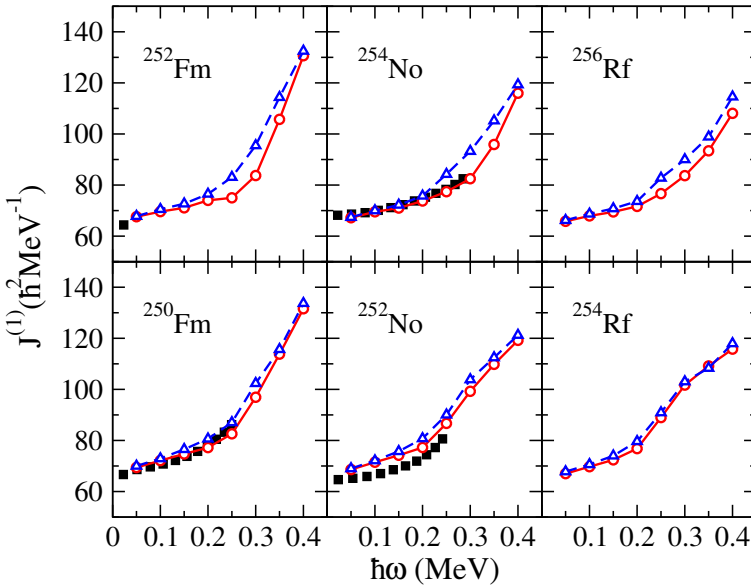


Fig. 1. Comparisons in moments of inertia for $N = 152$ (top panels) and $N = 150$ (bottom panels) nuclei, calculated with (open circles) and without (open triangles) the high-order β_6 and β_8 deformations. The filled squares are for experimental values.

2.2. High- K fission isomers with highly elongated shapes in actinide nuclei

In actinide nuclei, there is a kind of metastable states that appear in the second well of the PES with a highly elongated shape having the major-to-minor axis ratio of about 2:1 (where the first well generates the ground state). The shape-trapping states decay mostly by spontaneous fission and hence are called fission isomers. The emergence of the second energy minimum is due to the special shell structure of nucleon orbits, where clear shell gaps exist at large deformation. We have performed configuration-constrained PES calculations for low-lying two-qp high- K states in the second well [27]. The K isomerism could increase the stability of an isomer against fission, which we called high- K fission isomer with the double isomerism of high- K and shape. We have investigated high- K fission isomers for nuclei ^{238}U , $^{236,238,242}\text{Pu}$ and $^{240,242,244}\text{Cm}$ in which there exist some experimental observations of the broken-pair excited isomers [28]. The high- K fission isomers were calculated to have highly elongated prolate shapes around $\beta_2 \approx 0.60\text{--}0.65$, with the details of configurations predicted [27]. These calculations should be useful for further studies of the highly deformed isomers. The experimental energies of the isomers are well reproduced by our calculations [27]. It has been found that broken-pair multi-qp excitations extend nuclear shape coexistence, *e.g.*, in $A \sim 190$ neutron-deficient mass region [29]. In neutron-deficient Pb isotopes, the ground states have spherical shape, while the studied 2-qp high- K states have well-deformed oblate shapes [29]. For neutron-deficient Po isotopes, the ground states can be spherical, prolate, or oblate, while all the investigated 2-qp high- K states are oblate [29].

2.3. Reflection-asymmetric deformations in heavy nuclei

With an improved PES calculation by including the reflection-asymmetric deformations of β_3 and β_5 in the Woods–Saxon potential [30], we have investigated possible octupole deformations in superheavy mass region. Calculations were done in a deformation space $(\beta_2, \beta_3, \beta_4, \beta_5)$. No static octupole deformation was found in their ground states of superheavy nuclei [31]. However, some of the heaviest nuclei have octupole-soft characteristic. Actinide nuclei have been known to have octupole deformation. We focused on octupole properties in even $^{220\text{--}230}\text{U}$ [32] where the octupole correlation has been expected with observed alternate-parity enhanced $E1$ transitions in rotational bands [33, 34]. Our calculations gave static octupole deformations for $^{222,224,226}\text{U}$ ground states [32]. The ^{222}U nucleus remains reflection-asymmetric up to high spins, while $^{224,226}\text{U}$ become axially symmetric prolate at a rotational frequency of $\hbar\omega \approx 0.3\text{ MeV}$. A phase transition from reflection-asymmetry to reflection-symmetry was suggested to occur at ^{228}U of uranium isotopes [32]. The near-proton-dripline nucleus ^{108}Te and

nuclei around were observed to have collective rotational bands with the octupole feature of $E1$ transitions [35, 36]. We have carried out the detailed TRS calculations focusing on $^{106,108}\text{Te}$, predicting that these two nuclei have reflection-symmetric prolate shapes at low spins and octupole deformation appears at rotational frequencies $\hbar\omega \approx 0.5\text{--}0.7\text{ MeV}$ [37].

2.4. Triaxial deformations in Ge and Se isotopes

The γ deformation breaks the axial symmetry of rotation, which leads to breaking down the conservation of the quantum number K that is the spin projection onto the symmetry axis in an axially symmetric shape. Non-axial γ deformation has been widely found in collective rotational states. Quest for stable triaxial shapes in ground states, with a maximum triaxial deformation $\gamma \approx 30^\circ$, is still a major theme in nuclear structure. An investigation employing the Skyrme–Hartree–Fock and Gogny–Hartree–Fock–Bogoliubov models pointed out that most of germanium isotopes are γ -soft in their ground states, but the calculations are sensitive to the choices of model parameters [38]. Experimentally, it is difficult to determine the γ deformation. When the axial symmetry breaks, one cannot determine at the same time the quadrupole deformation parameters of both β_2 and γ from the experimental $B(E2)$ value. It was suggested to use a sum-rule method to estimate the asymmetry from experimental electromagnetic transition matrix elements [39]. With the sum-rule approximation, in Refs. [39, 40] the asymmetry of about 70 even–even nuclei in $A \approx 50\text{--}80$ and $90\text{--}190$ have been estimated with available experimental $E2$ matrix elements. The most pronounced triaxiality in ground states was found in the nuclei of $^{70\text{--}76}\text{Ge}$ and $^{74\text{--}82}\text{Se}$ [40]. However, such an analysis is unable to distinguish whether the triaxiality is caused by real static γ deformation or dynamic γ softness [39, 40]. According to the works of Refs. [41, 42], one should not expect rigid triaxiality in the ground state of any nucleus.

Employing the TRS method, we have investigated the shapes of even Ge and Se isotopes [43]. For the ground states of germanium isotopes, the calculations give shape transitions from a $|\gamma| \approx 30^\circ$ triaxial shape in ^{64}Ge to nearly oblate shapes in $^{66\text{--}72}\text{Ge}$ and to a $|\gamma| = 30^\circ$ triaxial shape again in ^{74}Ge , and towards weakly deformed prolate shapes in $^{78,80}\text{Ge}$ [43]. This is in agreement with the possible existence of a shape transition around $N = 40$, as predicted in Ref. [44]. It is of special interest that the stable nucleus ^{74}Ge has a $\gamma = 30^\circ$ maximum triaxiality in the ground state. The TRS calculation shows that the triaxial minimum at $\beta_2 \approx 0.23$ and $\gamma \approx -30^\circ$ exists starting from the ground state up to a spin of $I \approx 18$ and keeps yrast to $I \approx 14$ [43]. However, it should be noted that the triaxial shape of ^{74}Ge is γ -soft in the ground state and at low spins. Figure 2 shows shape evolutions with

increasing rotational frequency for other even isotopes. We see that these Ge isotopes are also deformation-soft. $^{70,72}\text{Ge}$ keep well-deformed triaxial shapes with increasing frequency.

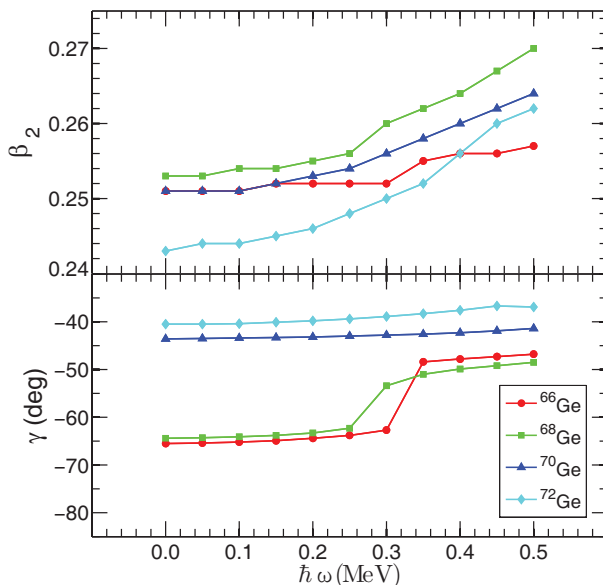


Fig. 2. Evolutions of calculated quadrupole deformations with increasing rotational frequency for even $^{66-72}\text{Ge}$ isotopes.

For selenium isotopes, $^{68-76}\text{Se}$ have large oblate deformations and a change into a weakly deformed prolate shape at ^{78}Se [43]. This is consistent with the experimental suggestions of well-deformed oblate shapes for the ground states in $^{68-74}\text{Se}$ [45–47]. The origin of the triaxiality has been analyzed by a plot of the Woods–Saxon single-particle orbits against the γ deformation. There exists a deformed $\gamma \approx 30^\circ$ shell at $Z(N) = 32$ [43]. At $Z(N) = 34$, however, an oblate shell appears, which would be the reason why ^{66}Ge ($N = 34$) and $^{68-76}\text{Se}$ ($Z = 34$) become oblate [43]. In general, though maximum triaxiality $|\gamma| = 30^\circ$ was found in Ge isotopes, the triaxial shapes are γ -soft, resulting in significant dynamical triaxial effects.

2.5. Triaxial strong deformation in ^{158}Er at ultrahigh spins

^{158}Er is a textbook nucleus for high-spin study. It exhibits various shapes with increasing the angular momentum of rotation, evolving from collective prolate to non-collective oblate to triaxial strong deformation (TSD) [11]. Three rotational alignments at spins $I \sim 10, 26$ and 38 have been observed in the same nucleus [48–50], which would be a unique case so far. Also, band termi-

nating phenomenon was seen in the spin range of $I \approx 40\text{--}50$ at non-collective oblate shapes (see Ref. [11] and references therein). Recently, experiments have reached ultrahigh spins of about $65\hbar$ in ^{158}Er [11, 12]. The experiment measured a large transitional quadrupole moment $Q_t \sim 11\text{ eb}$ [12] at the ultrahigh spins, which should correspond to a large quadrupole deformation. Principal-axis-cranked (PAC) Nilsson calculations gave two TSD minima in the TRS with one positive and another negative γ deformations in the ultrahigh-spin range [12]. At the lowest minimum TSD1 with positive γ , the PAC calculation gave $Q_t \sim 7.5\text{ eb}$ significantly underestimating the observed value. This led to the suggestion that the observed ultrahigh-spin band may be associated with TSD2 at a negative γ or with TSD3 which has a large quadrupole deformation [12]. For a triaxial shape, the rotational axis may not be in one of the principal axes.

In a recent work [51], we used both the Nilsson shell-correction tilted-axis cranking (SCTAC) [52] and for the first time the three-dimension self-consistent Skyrme–Hartree–Fock (SHF) tilted-axis cranking (SHFTAC) [53] to investigate the observed ultrahigh-spin band. The descriptions of numerical calculations of these two approaches can be found in Ref. [51]. In the SCTAC calculations, if we assume that the axis of rotation is in one of the principal axes (*i.e.*, principal axis cranking) we obtain the lowest triaxial minimum TSD1 at $(\beta_2 = 0.33, \gamma = 22^\circ)$ which is a rotation about the short axis and the second TSD2 at $(\beta_2 = 0.31, \gamma = -15^\circ)$ for a rotation about the medium axis [51], agreeing with the results of Ref. [12]. If we allow the rotational axis to tilt, however, the PAC minimum at $\gamma = -15^\circ$ becomes a saddle [51]. Therefore, TSD2 does not exist in fact. But TSD1 gives $Q_t \sim 8\text{ eb}$ which is too small as compared with the experimental value of $\sim 11\text{ eb}$ [12].

In the SCTAC method, the tilt angle of the rotational axis is defined relative to one of principal axes, which is a straightforward way. In SHFTAC, the tilted cranking is introduced by means of a constraint on the orientation of J along with the constraints $\text{Im}(Q_{22}) = Q_{2\pm 1} = 0$ on the orientation of the principal axis of the nucleus defined in terms of total (mass) quadrupole moment $Q_{2\mu}$. In Ref. [51], we have performed the self-consistent tilted-axis-cranking SHF calculations with two sets of Skyrme parameters SkM* and Sly4_L for four different configurations of ^{158}Er in the ultrahigh-spin range of $I \approx 40\text{--}70$. The SHFTAC calculations give consistent results with the SCTAC [51] for the lowest configuration. In addition, the SHFTAC calculation brings an excited configuration (indicated by “D” in Fig. 3) which has larger mass quadrupole deformation: $Q_{20} \approx 29\text{ b}$ and $Q_{22} \approx -6\text{ b}$, giving $\gamma = -\arctan(Q_{22}/Q_{20}) \approx 12^\circ$ [51], leading to a large charge transitional quadrupole moment $Q_t \approx 10.5\text{ eb}$ which is well close to the experimental value of $\approx 11\text{ eb}$. The calculations of tilted cranking total Routhians for the

excited TSD configuration “D” are given in Fig. 3. It is seen that the excited TSD configuration has a stable minimum at a tilt angle of $\theta = 0^\circ$ (a rotation about the short axis) while it is unstable with respect to a reorientation of the rotational axis. Further theoretical study would be needed for a full understanding of the experimental observation including the energies of the ultrahigh-spin states.

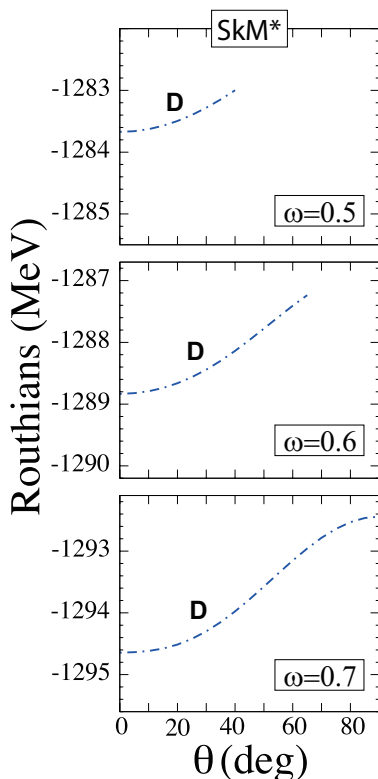


Fig. 3. Tilted cranking total Routhians of the excited TSD configuration “D” as a function of the tilt angle θ of the rotational axis, at different rotational frequencies, calculated with the Skyrme force SkM*. A configuration in SHFTAC is defined by the number of states occupied in four parity-signature (π, ρ) blocks, see [54] for the detail. The excited TSD “D” has the configuration: $\nu[23, 23, 22, 22] \otimes \pi[17, 17, 17, 17]$.

3. Summary

We have employed various models to study nuclear deformations and incurred effects on the behaviors of nuclei. The investigation based on the Woods–Saxon potential with the inclusion of high-order deformations shows

that the multipolarity-six, β_6 , deformation plays an important role in superheavy mass region. The β_6 deformation leads to the enlarged $Z = 100$ and $N = 152$ deformed shell gaps, which increases the stabilities of superheavy nuclei. The Woods–Saxon TRS calculations reproduce well the observed collective rotational bands of superheavy nuclei. The β_6 deformation can explain the delayed rotational alignments observed in even–even superheavy nuclei with $N \geq 152$ (compared with the alignments with $N < 150$). The effect from the β_6 deformation has also been seen in broken-pair multi-qp excitations. The configuration-constrained PES calculations with the inclusion of the β_6 deformation can remarkably improve the calculations of excitation energies of the observed isomeric states. The energies are sensitive to the level spacing of single-particle orbits.

Further, the configuration-constrained PES calculation has been applied to the investigation of multi-qp high- K isomeric states of actinide nuclei in the second well of the PES with highly elongated shapes at $\beta_2 \approx 0.60$ – 0.65 . The K isomerism plus shape trapping may cause the double isomerism against spontaneous fission, called high- K fission isomer. Our calculations reproduced well available experimental observations about high- K fission isomers, and predicted many possible high- K isomeric states in the second well. It is calculated that broken-pair multi-qp excitations can extend shape coexistence in $A \sim 190$ neutron-deficient nuclei, driving nuclei from sphere to be oblate in neutron-deficient Pb isotopes.

Based on the Woods–Saxon potential, the reflection-asymmetric deformations of β_3 and β_5 have been investigated for superheavy, actinide and near-proton-dripline Te nuclei. No static octupole deformation was found in their ground states of superheavy nuclei, while it appears in $^{222,224,226}\text{U}$ ground states and possibly in high-spin states. The TRS calculations predict that $^{106,108}\text{Te}$ might have reflection-symmetric prolate shapes at low spins and octupole correlation appears at certain rotational frequencies. Triaxiality in atomic nuclei is an important deformation degree of freedom. Using TRS method based on the Woods–Saxon potential, germanium isotopes are found to have triaxial deformation with a maximum triaxiality $\gamma \approx 30^\circ$ in ^{74}Ge . Selenium isotopes are more likely to be γ soft. To understand the observed large transitional quadrupole moment of ultrahigh-spin states in ^{158}Er , we have performed the sophisticated tilted-axis-tilting calculations based on the Nilsson and Skyrme–Hartree–Fock models. It is found that the second TSD minimum at negative γ deformation which appears in the PAC approach is a saddle point if allowing the rotational axis to tilt. An excited TSD configuration which appears at $\gamma \approx 12^\circ$ in the tilted-axis-tilting Skyrme–Hartree–Fock calculation can well reproduce the observed large quadrupole moment.

Valuable discussions with W. Nazarewicz, J. Dobaczewski and R. Wyss are gratefully acknowledged. These works have been supported by the National Key Basic Research Program of China under Grant 2013CB834400, and the National Natural Science Foundation of China under Grant Nos. 11235001, 11205120 and 10975006, the UK STFC, U.S. Department of Energy under Contracts No. DE-FG02-96ER40963 (University of Tennessee) and No. DE-FG02-95ER40934 (University of Notre Dame), Academy of Finland and the University of Jyväskylä within the FIDIPRO program.

REFERENCES

- [1] N. Tajima, N. Suzuki, *Phys. Rev.* **C64**, 037301 (2001).
- [2] A.N. Andreyev *et al.*, *Nature* **405**, 430 (2000).
- [3] A. Bohr, B.R. Mottelson, *Nuclear Structure*, Benjamin, New York 1975, Vol. 2.
- [4] S. Frauendorf, *Rev. Mod. Phys.* **73**, 463 (2001).
- [5] R. Bengtsson, H. Frisk, F.R. May, J.A. Pinston, *Nucl. Phys.* **A415**, 189 (1984).
- [6] F.R. Xu, W. Satula, R. Wyss, *Nucl. Phys.* **A669**, 119 (2000).
- [7] Y.H. Zhang *et al.*, *Phys. Rev.* **C68**, 054313 (2003).
- [8] P.A. Butler, W. Nazarewicz, *Rev. Mod. Phys.* **68**, 349 (1996).
- [9] H.L. Liu, F.R. Xu, P.M. Walker, C.A. Bertulani, *Phys. Rev.* **C83**, 011303 (2011).
- [10] H.L. Liu, F.R. Xu, P.M. Walker, *Phys. Rev.* **C86**, 011301(R) (2012).
- [11] E.S. Paul *et al.*, *Phys. Rev. Lett.* **98**, 012501 (2007).
- [12] X. Wang *et al.*, *Phys. Lett.* **B702**, 127 (2011).
- [13] S. Cwiok, P.-H. Heenen, W. Nazarewicz, *Nature* **433**, 705 (2005).
- [14] Z. Ren, *Phys. Rev.* **C65**, 051304 (2002).
- [15] P. Reiter *et al.*, *Phys. Rev. Lett.* **82**, 509 (1999).
- [16] Z. Patyk, A. Sobiczewski, *Nucl. Phys.* **A533**, 132 (1991).
- [17] Z. Patyk, A. Sobiczewski, *Phys. Lett.* **B256**, 307 (1991).
- [18] I. Muntian, Z. Patyk, A. Sobiczewski, *Phys. Lett.* **B500**, 241 (2001).
- [19] S. Eeckhauudt *et al.*, *Eur. Phys. J.* **A26**, 227 (2005).
- [20] R.-D. Herzberg *et al.*, *Nature* **442**, 896 (2006).
- [21] S.K. Tandel *et al.*, *Phys. Rev. Lett.* **97**, 082502 (2006).
- [22] P.T. Greenlees *et al.*, *Phys. Rev.* **C78**, 021303 (2008).
- [23] F.R. Xu, P.M. Walker, J.A. Sheikh, R. Wyss, *Phys. Lett.* **B435**, 257 (1998).
- [24] R.M. Clark *et al.*, *Phys. Lett.* **B690**, 19 (2010).
- [25] R.-D. Herzberg *et al.*, *Phys. Rev.* **C65**, 014303 (2001).

- [26] F.R. Xu, W. Satula, R. Wyss, *Nucl. Phys.* **A669**, 119 (2000).
- [27] H.L. Liu *et al.*, *Eur. Phys. J.* **A47**, 135 (2011).
- [28] B. Singh, R. Zywina, R.B. Firestone, *Nucl. Data Sheets* **97**, 241 (2002).
- [29] Y. Shi, F.R. Xu, H.L. Liu, P.M. Walker, *Phys. Rev.* **C82**, 044314 (2010).
- [30] W. Nazarewicz, S.L. Tabor, *Phys. Rev.* **C45**, 2226 (1992).
- [31] H.L. Wang, H.L. Liu, F.R. Xu, C.F. Jiao, *Chin. Sci. Bull.* **57**, 1761 (2011).
- [32] H.L. Wang, H.L. Liu, F.R. Xu, *Phys. Scr.* **86**, 035201 (2012).
- [33] P.T. Greenless *et al.*, *J. Phys. G* **24**, L63 (1998).
- [34] S. Zhu *et al.*, *Phys. Rev.* **C81**, 041306 (2010).
- [35] G.J. Lane *et al.*, *Phys. Rev.* **C57**, 1022 (1998).
- [36] G. de Angelis *et al.*, *Phys. Lett.* **B437**, 236 (1998).
- [37] H.L. Wang, H.L. Liu, F.R. Xu, C.F. Jiao, *Prog. Theor. Phys.* **128**, 363 (2012).
- [38] L. Guo, J.A. Maruhn, P.-G. Reinhard, *Phys. Rev.* **C76**, 034317 (2007).
- [39] W. Andrejtscheff, P. Petkov, *Phys. Rev.* **C48**, 2531 (1993).
- [40] W. Andrejtscheff, P. Petkov, *Phys. Lett.* **B329**, 1 (1994).
- [41] S. Åberg, H. Flocard, W. Nazarewicz, *Annu. Rev. Nucl. Part. Sci.* **40**, 439 (1990).
- [42] N.V. Zamfir, R.F. Casten, *Phys. Lett.* **B260**, 265 (1991).
- [43] S.F. Shen, S.J. Zheng, F.R. Xu, R. Wyss, *Phys. Rev.* **C84**, 044315 (2011).
- [44] R. Lecomte *et al.*, *Phys. Rev.* **C22**, 2420 (1980).
- [45] S.M. Fischer *et al.*, *Phys. Rev. Lett.* **84**, 4064 (2000).
- [46] T. Mylæus *et al.*, *J. Phys. G* **15**, L135 (1989).
- [47] P.D. Cottle *et al.*, *Phys. Rev.* **C42**, 1254 (1990).
- [48] R.M. Lieder *et al.*, *Z. Physik* **257**, 147 (1972).
- [49] I.Y. Lee *et al.*, *Phys. Rev. Lett.* **38**, 1454 (1977).
- [50] J. Burde *et al.*, *Phys. Rev. Lett.* **48**, 530 (1982).
- [51] Y. Shi *et al.*, *Phys. Rev. Lett.* **108**, 092501 (2012).
- [52] S. Frauendorf, *Nucl. Phys.* **A557**, 259 (1993); *Nucl. Phys.* **A677**, 115 (2000).
- [53] P. Olbratowski, J. Dobaczewski, J. Dudek, W. Plociennik, *Phys. Rev. Lett.* **93**, 052501 (2004).
- [54] J. Dobaczewski, J. Dudek, *Comput. Phys. Commun.* **131**, 164 (2000).